Mon. Not. R. Astron. Soc. **000**, 1–10 (2004) Printed 5 February 2008 (MN LATEX style file v2.2)

Star formation rates and chemical abundances of emission line galaxies in intermediate-redshift clusters

M. Mouhcine[1⋆], S.P. Bamford[2]†, A. Aragón-Salamanca[2], O. Nakamura[2]
[1] *Astrophysics Research Institute, Liverpool John Moores University, Twelve Quays House, Egerton Wharf, Birkenhead, CH41 1LD, UK.*
[2] *School of Physics and Astronomy, University of Nottingham, Nottingham, NG7 2RD, UK.*

Accepted ?. Received ?; in original form ?

ABSTRACT

We examine the evolutionary status of luminous, star-forming galaxies in intermediate-redshift clusters by considering their star formation rates and the chemical and ionsiation properties of their interstellar emitting gas. Our sample consists of 17 massive, star-forming, mostly disk galaxies with $M_B \lesssim -20$, in clusters with redshifts in the range $0.31 \lesssim z \lesssim 0.59$, with a median of $\langle z \rangle = 0.42$. We compare these galaxies with the identically selected and analysed intermediate-redshift field sample of Mouhcine et al. (2006), and with local galaxies from the Nearby Field Galaxy Survey of Jansen et al. (2000).

From our optical spectra we measure the equivalent widths of [OII]λ3727, Hβ and [OIII]λ5007 emission lines to determine diagnostic line ratios, oxygen abundances, and extinction-corrected star formation rates. The star-forming galaxies in intermediate-redshift clusters display emission line equivalent widths which are, on average, significantly smaller than measured for field galaxies at comparable redshifts. However, a contrasting fraction of our cluster galaxies have equivalent widths similar to the highest observed in the field. This tentatively suggests a bimodality in the star-formation rates per unit luminosity for galaxies in distant clusters. We find no evidence for further bimodalities, or differences between our cluster and field samples, when examining additional diagnostics and the oxygen abundances of our galaxies. This maybe because no such differences exist, perhaps because the cluster galaxies which still display signs of star-formation have recently arrived from the field. In order to examine this topic with more certainty, and to further investigate the way in which any disparity varies as a function of cluster properties, larger spectroscopic samples are needed.

Key words: galaxies: evolution – galaxies: abundances – galaxies: fundamental parameters – galaxies: clusters: general

1 INTRODUCTION

One of the central problems in astronomy is that of galaxy formation and evolution: when were the visible parts of galaxies assembled, when were the stars formed, and how did this depend on environment?

At low redshift the dependence of galaxy properties on environment is well established. Dense environments contain a larger fraction of red, passive galaxies, while low density environments show more blue, star-forming galaxies (e.g., Lewis et al. 2002; Gómez et al. 2003, Balogh et al. 2004). Furthermore, star-forming cluster galaxies tend to have lower rates of star formation than those in the field (Moss & Whittle 1993, 2000). These star formation patterns are accompanied by a morphological trend, such that denser regions have a larger fraction of early-types than the field (Morgan 1961, Dressler 1980). However, the origin of these environmental dependences is not yet clear, and continues to be debated.

As well as the local variation in galaxy properties with environment, there are differences between the galaxy populations observed in comparable environments at different cosmic epochs. In intermediate-redshift clusters there are a higher fractions of blue (Butcher & Oemler 1978, 1984), star-forming (Couch & Sharples 1987, Dressler & Gunn 1992, Poggianti et al. 1999), and spiral (Dressler et al. 1997) galaxies than in comparable local clusters. The integrated star for-

⋆ Isaac Roberts Fellow
† Current address: Institute of Cosmology and Gravitation, University of Portsmouth, Mercantile House, Hampshire Terrace, Portsmouth, PO1 2EG, UK.

mation rate per cluster mass is thus larger for higher redshift clusters (Finn et al. 2005, Homeier et al. 2005). However, the field also evolves substantially with redshift (e.g., Cowie et al. 1997), and intermediate-redshift cluster galaxies still always tend to have lower star formation rates (Balogh et al. 1998), star-forming fractions (Postman et al. 2001, Poggianti et al. 2006) and spiral fractions (Dressler et al. 1997) than field galaxies at the same epoch.

Recently the Tully-Fisher relation (Tully & Fisher 1977) has been used to investigate the differential evolution of cluster versus field galaxies at intermediate redshift. This method effectively utilizes rotation velocity, a proxy for total mass, as a baseline against which other galaxy properties, in this case luminosity, can be compared for different samples. Ziegler et al. (2003) have concluded that cluster galaxies at $z = 0.3$–0.5 are distributed in the Tully-Fisher diagram similarly to field galaxies at the same redshifts, suggesting that the mass-to-light ratios of cluster galaxies are not affected by physical processes specific to high density regions. In contrast, Milvang-Jensen et al. (2003) found mild evidence that cluster galaxies are brighter than field ones at a fixed rotation velocity. Using a larger sample, Bamford et al. (2005) also found that for luminous, star-forming field and cluster disc galaxies at $0.3 \lesssim z \lesssim 0.8$, the cluster galaxies are systematically brighter with respect to the Tully-Fisher relation of the field at the 3σ level. They speculate that this might be due to the increased presence of young stellar populations in galaxies which have recently entered the cluster environment, due to an enhancement of star formation caused by some interaction with that environment. However, Nakamura et al. (2006) fail to confirm this cluster–field offset with a comparable sample. The question is therefore not yet settled, and awaits the results from much larger studies, such as the ESO Distant Cluster Survey (EDisCS; White et al. 2005) and the Deep Extragalactic Exploratory Probe 2 (DEEP2; Davis et al. 2003).

The degree of chemical enrichment in distant star-forming galaxies provides insight into how populations of distant galaxies map onto those in the local universe. Analyses of the oxygen abundances of star-forming field galaxies at intermediate redshifts seem to indicate that the luminosity–metallicity relation evolves with redshift, with steeper slope (faster variation in metallicity with luminosity) at earlier cosmic times (Kobulnicky et al. 2003; Maier et al. 2004; Liang et al. 2004). These studies imply that lower luminosity field galaxies have experienced substantial chemical evolution since $z \sim 1$, while the brightest galaxies have changed little. Mouhcine et al. (2006) found that the properties of the interstellar star-forming gas for a sample of luminous, massive field galaxies at $0.2 \lesssim z \lesssim 0.8$ cover a wide range, extending from those observed for local bright galaxies to those of local dwarf galaxies. A subsample of these galaxies have already undergone significant chemical enrichment, as indicated by their high oxygen abundances. However, at a given galaxy luminosity many field galaxies have oxygen abundances, $12 + \log(\mathrm{O/H}) \sim 8.6$, significantly lower than local galaxies with similar luminosities. These galaxies exhibit physical conditions, i.e., emission line equivalent width and ionization state, very similar to those of local *faint*, metal-poor, star-forming galaxies.

In this paper, we analyze star formation rates and the properties of the interstellar emitting gas for a sample of 17 intermediate redshift cluster galaxies. Seven of these have securely measured rotation velocities and emission scale lengths. The galaxies are drawn from the Bamford et al. (2005, 2006) and Nakamura et al. (2006) samples, which were primarily constructed to compare the Tully-Fisher relations of cluster and field galaxies at intermediate redshifts. We measure emission line equivalent widths, diagnostic ratios, and oxygen abundances for cluster galaxies, with the aim of investigating the environmental effects on the chemical content of galaxies at intermediate redshift. Even with a small sample of cluster galaxies, we are able to discern clear differences between intermediate redshift field and cluster galaxy properties.

Table 1. Coordinates and membership of cluster galaxies in our sample

ID	R.A. (J2000)	Dec. (J2000)	Cluster
1	02:39:54.4	-01:33:35	A 370
2	02:39:46.4	-01:32:17	A 370
3	02:39:59.2	-01:35:03	A 370
4	22:58:34.0	-34:46:52	AC 114
5	22:58:40.6	-34:50:12	AC 114
6	22:58:46.3	-34:46:43	AC 114
7	22:58:49.3	-34:47:01	AC 114
8	00:56:48.4	-27:40:03	CL 0054-27
9	20:56:22.7	-04:35:54	MS 2053.7-0449
10	00:18:31.1	16:22:05	MS 0015.9+1609
11	00:18:26.2	16:25:08	MS 0015.9+1609
12	00:18:30.9	16:25:41	MS 0015.9+1609
13	00:18:29.2	16:23:12	MS 0015.9+1609
14	16:23:42.3	26:30:55	MS 1621.5+2640
15	16:23:39.1	26:36:15	MS 1621.5+2640
16	16:23:38.0	26:35:40	MS 1621.5+2640
17	16:23:41.5	26:35:37	MS 1621.5+2640

The paper is organized as follows. In Section 2 we briefly describe the sample selection and emission line measurements. In Section 3, we discuss the differences in ionization condition, luminosity–metallicity relation, and star formation rates for cluster galaxies at intermediate redshifts with respect to both intermediate redshift and local field samples. Our results are summarised, and their implications briefly discussed, in Section 4.

A concordance cosmological model with $\mathrm{H_0} = 70\,\mathrm{km\,s^{-1}}$, $\Omega_\Lambda = 0.7$, $\Omega_m = 0.3$ has been adopted throughout the paper.

2 OBSERVATIONS AND SAMPLE SELECTION

The observed galaxies are located in nine fields, centered on the clusters MS 0440.5+0204 ($\mathrm{z_{cl}} = 0.20, \sigma_{\mathrm{cl}} = 838\mathrm{kms^{-1}}$), A 2390 ($\mathrm{z_{cl}} = 0.23, \sigma_{\mathrm{cl}} = 1294\mathrm{kms^{-1}}$), AC 114 ($\mathrm{z_{cl}} = 0.32, \sigma_{\mathrm{cl}} = 1388\mathrm{kms^{-1}}$), A 370 ($\mathrm{z_{cl}} = 0.37, \sigma_{\mathrm{cl}} = 859\mathrm{kms^{-1}}$), MS 1621.5+2640 ($\mathrm{z_{cl}} = 0.43, \sigma_{\mathrm{cl}} = 735\mathrm{kms^{-1}}$), MS 0015.9+1609 ($\mathrm{z_{cl}} = 0.55, \sigma_{\mathrm{cl}} = 984\mathrm{kms^{-1}}$), CL 0054-27 ($\mathrm{z_{cl}} = 0.56, \sigma_{\mathrm{cl}} = 742\mathrm{kms^{-1}}$), MS 2053.7-0449 ($\mathrm{z_{cl}} = 0.58, \sigma_{\mathrm{cl}} = 817\mathrm{kms^{-1}}$), and MS 1054.4-0321 ($\mathrm{z_{cl}} = 0.83, \sigma_{\mathrm{cl}} = 1178\mathrm{kms^{-1}}$), where z_{cl} and σ_{cl} cluster redshifts and velocity-dispersions, obtained from the literature (Stocke et al. 1991; Girardi & Mezzetti

Table 2. Properties of our sample of intermediate redshift cluster galaxies. The columns give the ID, redshift, absolute rest-frame B-band magnitude, rest-frame equivalent widths of [OII]λ3727, Hβ and [OIII]λ5007, rotation velocity, emission scalelength, star formation rate determined from Hβ, and the colour excess due to internal dust extinction, respectively.

ID	z	M_B mag	EW([OII]λ3727) (Å)	EW(Hβ) (Å)	EW([OIII]λ5007) (Å)	V_{rot} (kms^{-1})	size (kpc)	12 + log(O/H)	SFR() (M$_\odot$yr^{-1})	E(B-V) (mag)
1	0.373	-22.03 ± 0.13	16.6 ± 0.5	12.8 ± 0.3	1.0 ± 0.2	...	...	9.02 ± 0.01	9.23 ± 0.23	0.12 ± 0.04
2	0.378	-21.13 ± 0.17	30.3 ± 1.8	5.1 ± 0.9	4.9 ± 0.7	247. ± 11.	7.7 ± 0.3	8.41 ± 0.21	1.62 ± 0.28	0.000 ± 0.31
3	0.384	-20.46 ± 0.1	26.8 ± 1.5	6.3 ± 0.6	7.2 ± 0.6	...	...	8.58 ± 0.09	1.08 ± 0.10	0.000 ± 0.18
4	0.306	-20.72 ± 0.08	13.7 ± 0.9	2.1 ± 0.3	1.6 ± 0.4	$81._{+23.}^{-16.}$	$4.3_{+0.2}^{-0.3}$	...	...	...
5	0.313	...	19.6 ± 1.8	7.4 ± 1.	5.6 ± 0.8	...	...	8.79 ± 0.07	...	...
6	0.312	-21.09 ± 0.08	12.2 ± 0.6	3.5 ± 0.2	4.8 ± 0.2	...	...	8.64 ± 0.04	1.07 ± 0.05	0.14 ± 0.09
7	0.313	-21.26 ± 0.08	6.7 ± 0.9	4.4 ± 0.6	4.3 ± 0.2	$85._{+15.}^{-13.}$	3. ± 0.6	8.89 ± 0.04	1.56 ± 0.23	0.51 ± 0.22
8	0.559	-21.06 ± 0.12	26.2 ± 1.8	22.7 ± 1.5	3.5 ± 1.6	194. ± 35.	2.5 ± 0.4	9.03 ± 0.01	6.74 ± 0.44	0.21 ± 0.11
9	0.588	-20.38 ± 0.1	63.8 ± 3.8	25.6 ± 2.7	16.2 ± 1.7	...	...	8.83 ± 0.05	4.07 ± 0.43	0.000 ± 0.16
10	0.551	-21.34 ± 0.1	11.9 ± 1.3	3.2 ± 1.0	4.1 ± 0.9	...	...	8.63 ± 0.26	1.24 ± 0.39	0.21 ± 0.53
11	0.554	-20.89 ± 0.09	7.6 ± 2.8	5.2 ± 1.3	3.2 ± 1.6	...	...	8.94 ± 0.05	1.32 ± 0.33	0.69 ± 0.47
12	0.549	-22.28 ± 0.08	23.9 ± 0.9	4.1 ± 0.8	2.2 ± 0.5	...	...	8.43 ± 0.24	3.67 ± 0.73	0.000 ± 0.35
13	0.550	-20.44 ± 0.11	19.6 ± 1.9	6.9 ± 1.2	5.3 ± 2.5	$137._{+49.}^{-37.}$	$4.6_{+0.5}^{-0.4}$	8.77 ± 0.11	1.16 ± 0.20	0.10 ± 0.30
14	0.424	-21.15 ± 0.07	10.5 ± 1.0	4.9 ± 0.8	5.4 ± 0.4	$213._{+7.}^{-6.}$	$2.7_{+0.1}^{-0.2}$	8.81 ± 0.07	1.56 ± 0.26	0.49 ± 0.25
15	0.422	-20.93 ± 0.09	63.2 ± 1.6	21.7 ± 1.	19.6 ± 0.7	...	...	8.75 ± 0.03	5.71 ± 0.25	0.000 ± 0.07
16	0.421	-20.75 ± 0.08	24.5 ± 1.6	7.9 ± 0.9	6.9 ± 0.7	$216._{+19.}^{-16.}$	$3.2_{+0.3}^{-0.3}$	8.73 ± 0.08	1.76 ± 0.21	0.09 ± 0.19
17	0.429	-19.97 ± 0.08	14.1 ± 2.7	6.2 ± 1.5	3.3 ± 1.3	...	...	8.86 ± 0.09	0.67 ± 0.16	0.09 ± 0.38

2001; Hoekstra et al. 2002). Spectroscopy and imaging were obtained using FORS2[1] on the VLT (Seifert et al. 2000), for MS 0440.5+0204, AC 114, A 370, CL 0054-27, MS 2053.7-0449, MS 1054.4-0321, and using FOCAS[2] on the Subaru telescope (Kashikawa et al. 2002) for A 2390, MS 1621.5+2640, MS 0015.9+1609, MS 2053.7-0449 again. The cluster galaxies considered in this paper are defined as those galaxies with redshifts, z, such that $z_{\rm cl} - 3\sigma_{\rm cl} \leqslant z \leqslant z_{\rm cl} + 3\sigma_{\rm cl}$. Galaxies with redshifts outside of these limits were assigned to the field sample considered in Mouhcine et al. (2006).

As the original samples were designed to study the Tully-Fisher relation, the galaxies observed within each field were selected by assigning priorities based upon the likelihood of being able to measure a rotation curve. Galaxies with disky morphologies, favourable inclination for rotation velocity measurement, known emission line spectrum, and available Hubble Space Telescope data were assigned higher priorities. The sample is thus biased toward luminous, star-forming disc galaxies, and therefore we are not probing the average galaxy population in clusters.

The reduction of the spectroscopic and photometric data are detailed in Bamford et al. (2005) and Nakamura et al. (2006), and summarised in Mouhcine et al. (2006). The products utilized in this paper are wavelength-calibrated, sky-subtracted, non-flux-calibrated 1d-spectra spanning the observed range $\sim$ 5000–8500 Å at 4.2–6.3 Å resolution (FWHM), from spatial regions covering the whole major axis of each galaxy, and absolute rest-frame B-band total magnitudes.

To measure emission line equivalent widths, single Gaussian fits were attempted for all visible emission lines. Balmer emission lines were corrected for the underlying stellar absorption by considering simultaneous fits of the emission and absorption lines. For a fraction of the galaxy spectra, particularly with low S/N, these two-component fits were found to be unreliable. To correct the affected galaxies, we thus apply a uniform stellar absorption correction estimated from the galaxies with both reliable two- and one-component fits (see Mouhcine et al. 2006 for more details).

Our initial sample of cluster galaxies with identifiable emission lines contains 72 galaxies, and spans a redshift range of 0.2 to 0.84 with a median of 0.55. We searched within this spectroscopic sample for galaxies with emission lines suitable for chemical analysis. Only galaxies for which it was possible to measure [OII]λ3727, Hβ, and [OIII]λ5007 emission lines were retained, i.e., the lines needed to determine the ionizing source and to measure the oxygen abundance. After applying these selection criteria the sample size drops to 22. For reliable oxygen abundance determinations, only galaxies for which Hβ emission line is well detected are retained. This was judged by requiring the S/N, estimated from the median pixel value in regions 29–58Å away from the line on both sides, divided by the median value of the error image in the same region, to be larger than 8. An additional 5 objects were excluded from the sample due to the weak detection of Hβ. Of the the original data set with 72 objects, the final sample contains 17 emission line galaxies in the redshift range $0.31 \lesssim z \lesssim 0.59$, with a median of $\langle z \rangle = 0.42$. These galaxies span almost 2.5 magnitude in B-band luminosity ($M_B = -19.9$ to -22.3), with a median of -21. Seven of the cluster galaxies in our sample have securely measured rotation velocities, in the range $V_{\rm rot} = 82$–248 kms^{-1} with a median of 194 kms^{-1}, and emission scale length in the range $r_{\rm d,spec} = 2.5$–7.7 kpc, with a median of 3.2 kpc (see Bamford et al. 2005 for more details on the measurements of rotation velocities and emission scale lengths). [3]

[1] http://www.eso.org/instruments/fors
[2] http://www.naoj.org/Observing/Instruments/FOCAS

[3] These numbers reduce to 16 galaxies with oxygen abundances (6 of which have measured $V_{\rm rot}$ & $r_{\rm d,spec}$), after we reject one galaxy due to difficulties in measuring its metallicity, and 15

The lower panel of Fig. 1 shows the relationship between rest-frame B-band absolute magnitude and redshift for the final cluster galaxy sample, shown as filled circles, and a comparison sample of intermediate redshift field galaxies from Mouhcine et al. (2006). The figure shows that the redshift and the galaxy luminosity are correlated for the comparison sample of field galaxies. No clear correlation is seen for our cluster galaxies, however the luminosities covered at a given redshift are consistent for the two samples.

The upper panel of the figure shows the redshift distribution for galaxies in our intermediate redshift cluster (hatched, thin line) and field (thick line) samples. Clearly, the bulk of field galaxies in the comparison sample are distributed over a redshift interval similar to our cluster galaxies. The redshift distribution of the field galaxies does, however, extend beyond that of our cluster galaxies.

For the high-redshift end of the distribution, we lose the [OIII]λ5007 emission line from the spectral range above $z \sim 0.7$, so that the final sample does not contain any galaxy from the most distant cluster (MS 1054.4-0321). Note that there is not a sharp redshift cutoff at which we lose the required lines, as the exact wavelength range of the spectra depend upon the position of the slit in the mask (see Bamford et al. 2005 and Nakamura et al. 2006 for more details).

A similar situation occurs at the low-redshift end of the distribution. We have a few field galaxies at $z \sim 0.2$, but no cluster galaxies due to the slightly different wavelength ranges of the VLT and Subaru data. For the VLT data the cutoff is setting in by $z \approx 0.2$, the redshift of MS0440. For Subaru data the cutoff occurs above $z = 0.23$, which is the reason why the final sample does not contain any galaxies from cluster A2390. We are also missing field galaxies at redshifts around the two clusters at $z_{\rm cl} = 0.55$ and $z_{\rm cl} = 0.56$ due to the presence of telluric atmospheric absorption at $\sim$ 7580–7700 Å. The spectra were not corrected for this feature, and so the lines which fell into this region were not used due to the difficulty in measuring their equivalent widths. This occurs for [OIII]λ5007 at $z = 0.514 - 0.538$ and for Hβ at $z = 0.559 - 0.584$. The cluster galaxy at $z \sim 0.559$ is just outside the affected range. It is worth mentioning that the results presented in this paper do not change if the field galaxies beyond the limits where cluster galaxies are detected are excluded from the intermediate redshift comparison sample.

An accurate estimate of the interstellar star-forming gas properties requires that the observed emission lines arise in HII regions, powered by photoionization from massive stars. None of the observed spectra contain all the required emission lines to determine the ionizing source using the classical techniques. Therefore, we use the equivalent width ratios of [OIII]λ4959, λ5007/Hβ and [OII]λ3727/Hβ as parametrized by Lamareille et al. (2004) to check the nature of the ionizing source. All the objects in our sample fall within the zone where starburst galaxies are located, indicating that for all of them the source ionizing the interstellar gas is an episode of star formation.

galaxies with star formation rates and internal dust reddenings (6 with $V_{\rm rot}$ & $r_{\rm d,spec}$) after we reject another galaxy with no magnitude measurement; see section 3.1

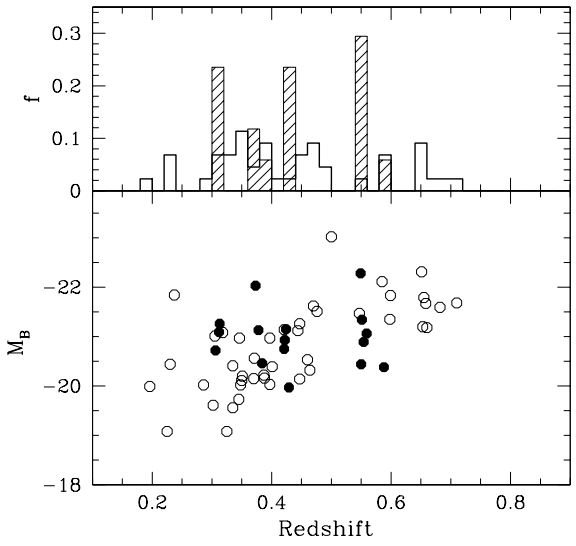

Figure 1. Lower panel: The relationship between B-band absolute magnitude and redshift for the sample of cluster galaxies, shown as field circles. The relationship for the comparison sample of field galaxies is shown as open circles. Upper panel: The redshift distribution for field and cluster galaxy samples shown are open and hatched histograms respectively.

3 PROPERTIES OF CLUSTER GALAXIES

3.1 Comparison samples & oxygen abundances

We take a step toward quantifying environmental variation in galaxy properties at intermediate redshifts by comparing our cluster galaxy properties with those of field galaxies from Mouhcine et al. (2006). The redshift distributions of both field and cluster galaxy samples are comparable, the field galaxies span a redshift range $0.2 \lesssim z \lesssim 0.8$ with a median of $\langle z \rangle = 0.45$. The comparison sample of intermediate redshift field galaxies was selected and analysed in an identical manner to the sample studied in this paper.

To investigate differences between the properties of $z \sim 0.5$ cluster galaxies and the general present day galaxy population, we require a local comparison sample. For this we use the sample of Jansen et al. (2000), who observed the Nearby Field Galaxy Survey (NFGS) of about 200 galaxies. The NFGS was selected from the first CfA redshift catalogue (Huchra et al. 1983) to approximate the local galaxy luminosity function. To select star-forming galaxies in the original NFGS sample, we use the classical diagnostic ratios of two pairs of relatively strong emission lines (Baldwin et al. 1981; Veilleux & Osterbrock 1987). The colour excess from obscuration by dust for NFGS sample galaxies was estimated from the observed ratio of Hα and Hβ line fluxes. We adopt the Milky Way interstellar extinction law of Cardelli, Clayton, & Mathis (1989), with $R_V = 3.1$, and assume an intrinsic Balmer decrement of 2.85, corresponding to the case B recombination with a temperature of $\rm T = 10^4 K$ and a density of $\rm n_e \sim 10^2 - 10^4\,cm^{-2}$ (Osterbrock 1989).

Gas phase oxygen abundances are estimated using the so-called strong emission line method, based on measurements of [OII]λ3727, [OIII]λ4959, λ5007, and Hβ (Mc-

Table 3. Statistical comparison of our cluster and field samples. For each parameter (x), the columns give the number of cluster and field objects (n_{cl} and n_f respectively), the robust mean of that parameter for cluster and field objects ($\overline{x}_{cl}$ and $\overline{x}_f$ respectively), the cluster−field difference in the means ($\Delta(\overline{x}_{cl} - \overline{x}_f)$), an estimate of the size of cluster−field difference that would be required in order to discriminate between the two at the 3σ-level ($|\Delta_{dis}| = 3 \times \sqrt{(\sigma^2_{\overline{x}_{cl}} + \sigma^2_{\overline{x}_f})}$), the probability that the cluster and field populations have the same mean ($P(\mu_{cl} = \mu_f)$), and the KS-test probability that the cluster and field population distributions are the same (P(KS)).

x	n_{cl}	n_f	$\overline{x}_{cl}$	$\overline{x}_f$	$\Delta(\overline{x}_{cl} - \overline{x}_f)$	$\lvert\Delta_{dis}\rvert$	$P(\mu_{cl}=\mu_f)$ %	P(KS) %
EW([OII]λ3727) (Å)	17	44	17.55 ± 2.68	33.86 ± 2.82	−16.31	11.68	0.013[a]	0.991
EW(Hβ) (Å)	17	44	5.35 ± 0.65	10.24 ± 0.82	−4.90	3.14	0.002[a]	1.826
O_{32}	17	44	0.35 ± 0.05	0.33 ± 0.03	0.02	0.17	75.63	96.53
R_{23}	17	44	4.13 ± 0.48	4.87 ± 0.30	−0.75	1.71	19.19	44.96
M_B (mag)	16	43	-20.90 ± 0.15	-20.79 ± 0.14	−0.11	0.61	57.34	19.87
SFR ($M_\odot\,yr^{-1}$)	15	39	1.34 ± 0.23	2.37 ± 0.38	−1.03	1.32	2.242[b]	46.45
$12 + \log(O/H)$	16	40	8.77 ± 0.05	8.71 ± 0.03	0.06	0.17	25.09	50.55
E(B−V) (mag)	15	39	0.10 ± 0.05	0.08 ± 0.01	0.03	0.16	61.53	74.35

[a] highly significant [b] significant, but see discussion in text for caveats.

Gaugh 1991). This is done through the parameter R_{23} = ([OIII]λ4959, λ5007+[OII]λ3727)/Hβ introduced initially by Pagel et al. (1979). The R_{23} parameter is both abundance- and ionization-sensitive (e.g., Kewley & Dopita 2002). The correction of this dependence of R_{23} parameter on ionization is usually done by using the ionization-sensitive diagnostic ratio O_{32} = [OIII]λ4959, λ5007/[OII]λ3727 (e.g., McGaugh 1991; Kewley & Dopita 2002). Note that the oxygen abundance estimated using different calibrations available in the literature might differ by factors up to ~ 4 (Ellison & Kewley 2005), however, as our main interest is to study the relative change in oxygen abundances between cluster and field galaxies, the exact choice of the $12 + \log(O/H)$ vs. R_{23} calibration is not a critical issue. Here we determine oxygen abundance using the calibration of McGaugh (1991), as taken from in Kobulnicky, Kennicutt & Pizagno (1999).

The use of R_{23} parameter to estimate oxygen abundance is complicated by the degenerate dependence of this parameter on metallicity: at the same value of R_{23}, different ionization parameters correspond to different oxygen abundances (McCall et al. 1985). The observed emission lines for our sample galaxy spectra are not enough to break the degeneracy. However, when the needed emission lines to do so are observed for intermediate redshift galaxies with similar luminosities, they are found to lie on the metal-rich branch of the $12 + \log(O/H)$ versus R_{23} calibration (Kobulnicky et al. 2003; Maier et al. 2005). To estimate the oxygen abundance, we make the assumption that the galaxies in our sample lie on the upper metallicity branch of the $12 + \log(O/H)$ versus R_{23} calibration. R_{23} and O_{32} have been estimated using emission line equivalent widths. Kobulnicky & Phillips (2003) have shown that estimates of both ratios using equivalent widths give results similar to using emission line fluxes.

For one galaxy in the sample, the oxygen abundance estimated using the low-branch of metallicity calibration, given its R_{23} and O_{32} parameters, was larger than that derived using the upper-branch. This occurs when the measured R_{23} parameter reaches a higher value than the maximum allowed by the photoionization model, i.e., for a given O_{32}. The estimate of oxygen abundance in this case is highly uncertain. No estimate of the oxygen abundance was made for this galaxy.

None of the objects in our sample have both Hα and Hβ emission lines present in their covered spectral range, so the dust obscuration cannot be derived using the Balmer decrement. However, it is possible to estimate the amount of internal extinction by comparing the energy balance between the luminosities of two different star formation indicators, [OII]λ3727 and Hβ in this case after applying the appropriate corrections, that are free from systematic effects other than dust reddening, i.e., that do not depend on the metallicity or excitation state of the emitting gas. The star formation rate in terms of the [OII]λ3727 emission line includes a correction factor to account for the effect of metallicity on the variation of the [OII]λ3727/Hα flux ratio, as calibrated by Kewley, Geller & Jansen (2004; see Mouhcine et al. 2005).

Table 2 lists the redshifts, absolute B-band magnitudes, [OII]λ3727, Hβ, and [OIII]λ5007 emission line rest-frame equivalent widths, rotation velocities, emission scale lengths, oxygen abundances, star formation rates, and colour excesses for the objects in our final sample of 17 cluster galaxies.

3.2 Results

The distributions of [OII]λ3727 and Hβ equivalent width, O_{32} and R_{23} parameters, M_B, star formation rate derived from Hβ, oxygen abundance, and colour excess are shown for our intermediate redshift cluster and field samples in Fig. 2. In addition to the visual comparison between our cluster and field samples afforded by these histograms, we have quantitatively compared the parameters. This has been done primarily by estimating the difference between the parameters' parent distribution means and evaluating the significance of this difference. The results are given in table 3. The figures presented in this table are from a comparison utilising robust biweight estimators (e.g., Beers, Flynn & Gebhardt 1990). The probability that the parent distributions have the same mean is evaluated by a robust t-test, which does not assume that the distributions have equal variances (Welch 1937). Similar results are found using canonical statistics, both unweighted and with weights corresponding to the measurement errors with the inclusion of an intrinsic dispersion term. An exception is $SFR_{H\beta}$, for which the less robust

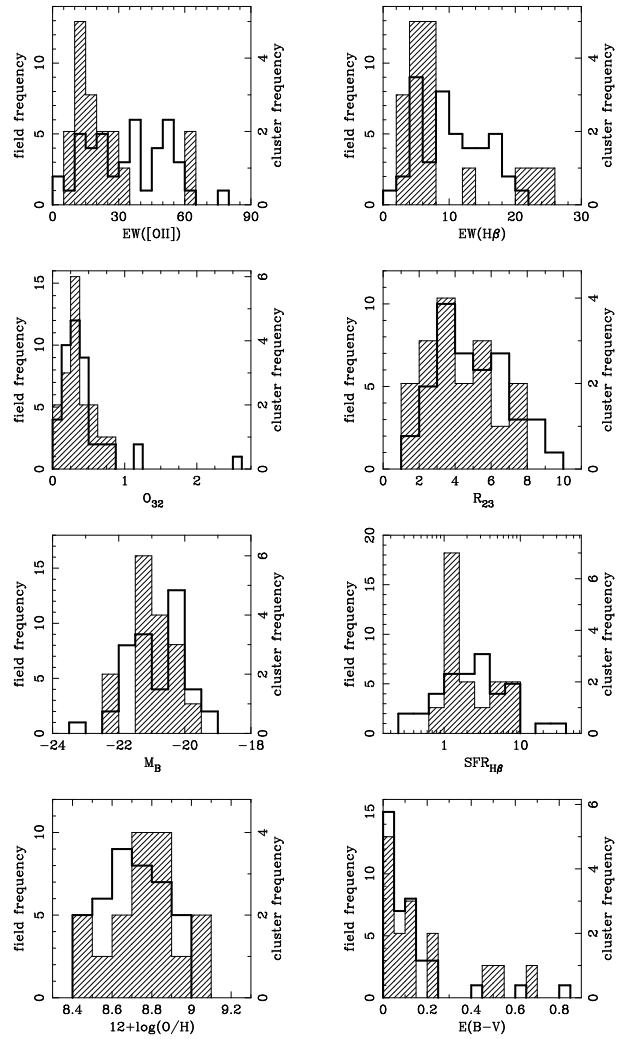

Figure 2. The distributions of [OII]λ3727 and Hβ equivalent width, the O_{32} and R_{23} parameters, M_B, star formation rate derived from Hβ (shown as $\log_{10}(\mathrm{SFR}_{\mathrm{H}\beta})$ to aid comparison), oxygen abundance, and colour excess for galaxies in our intermediate redshift cluster (hatched, thin line) and field (thick line) samples. The cluster and field histograms are plotted on different scales such that they both enclose the same area.

statistics find a less significant difference between the cluster and field samples. Table 3 also lists the probability that the parent cluster and field distributions are the same as given by a Kolmogorov-Smirnov (KS) test.

The most striking differences are displayed by the equivalent widths of [OII]λ3727 and Hβ, for which the cluster and field galaxy means differ at a $\gtrsim 99.99\%$ significance level. The KS-test also finds differences at a $> 98\%$ significance level. The equivalent widths of [OII]λ3727 and Hβ are on average significantly lower for cluster galaxies than for field galaxies in our samples, both by a factor of $\sim 0.52 \pm 0.09$. If there is no variation in broad-band luminosities (M_B) between these galaxy samples, these equivalent width ratios imply similar emission line luminosity ratios. Star formation rate is proportional to the Hβ luminosity and, upto a metallicity and ionisation dependence, to the [OII]λ3727 luminosity. We therefore expect the star formation rates of our cluster galaxies to be on average lower than those in our

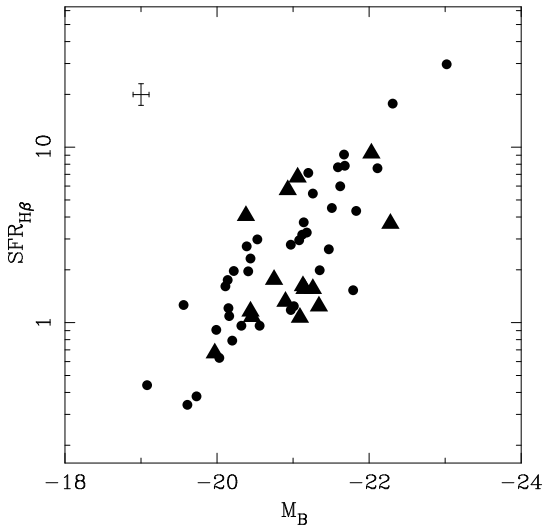

Figure 4. Magnitude versus star formation rate, derived from Hβ, for our samples of field (circles) and cluster (triangles) galaxies. Representative errors are shown by the error bars in the top left corner.

field sample, by a similar factor. Indeed, we find this to be true, by a factor of 0.6 ± 0.1. However, this result is less significant than that based solely upon the equivalent widths. The robust statistics presented in table 3 find the difference to be $\sim 98\%$, but canonical statistics and the KS-test find no significant difference. Also, if the comparison is performed in the log-regime, which may be more appropriate, no significant difference is found. This reduction in significance is probably due to broad-band luminosity variations. The spread in luminosity (~ 2 mag, therefore a factor of ~ 6 in luminosity) is comparable to the spread in equivalent width, and appears to blur out the differences between the cluster and field samples, reducing the significance of the difference, but not particularly affecting its magnitude.

However, these statistics do not tell the whole story. While most cluster galaxies have equivalent widths on the low side of the field distrib, there are several objects (10–20%) which have equivalent widths as high as any of the field galaxies. This bimodality is visible in Fig. 3 in the plot of [OII]λ3727 equivalent width versus B-band magnitude. It also remains in the star formation rate distribution, with the majority of our cluster galaxies having star formation rates at the low end of the field distribution, but with several objects ($\sim 20\%$) having SFRs higher than any of the field galaxies with the same broad-band luminosity. This is shown clearly by a plot of star formation rate versus magnitude, as given in Fig. 4. These results tentatively imply that distant cluster galaxies have a star formation rate per unit luminosity that is lower than the average for coeval field galaxies, with the exception of a subsample of $\sim 20\%$ cluster galaxies, which have star formation rates per unit luminosity that are higher than those usually seen in the field. We do not find evidence for bimodalities in the distribution histograms for any of the other parameters measured for our distant field and cluster galaxies.

Locally, the strength of emission lines is known to correlate with other galaxy properties, e.g., luminosity, metallicity, and ionization conditions (e.g., McCall et al. 1985;

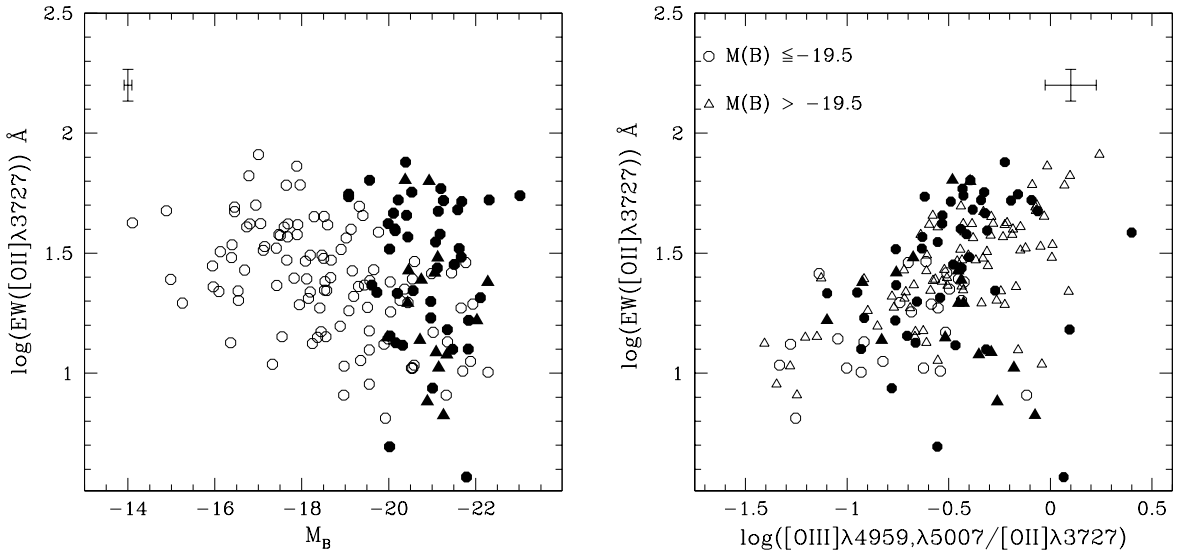

Figure 3. *Left*: The relationship between rest-frame [OII]λ3727 emission line equivalent width and absolute B-band magnitude for our samples of intermediate redshift bright, star-forming galaxies (field galaxies as filled circles, and cluster members as filled triangles), and the NFGS local star-forming galaxies (open circles). *Right*: Rest-frame [OII]λ3727 emission line equivalent width as a function of the excitation-sensitive diagnostic ratio O_{32}. Field star-forming galaxies at intermediate redshifts are shown as filled circles, and cluster members as filled traingles, open triangles show faint ($M_B > -19.5$) NFGS galaxies, and open circles show bright ($M_B > -19.5$) NFGS galaxies.

Stasińska 1990; Kewley & Dopita 2002; Mouhcine et al. 2005). On average faint/metal-poor galaxies tend to be highly ionized, while luminous/metal-rich galaxies are characterized by low-ionization parameters. The left panel of Fig. 3 shows the relationship between galaxy absolute B-band magnitude and [OII]λ3727 rest-frame emission line equivalent width. Our cluster galaxies are shown as filled triangles, the sample of intermediate redshift field galaxies from Mouhcine et al. (2006) is shown by filled circles, and the local star-forming galaxies in the NFGS sample are shown as open circles. The NFGS galaxies in this figure display the well-established correlation between galaxy luminosity and emission line equivalent width (e.g., Salzer et al. 1989; Kong et al. 2002; Jansen et al. 2000). As discussed in Mouhcine et al. (2006), the distant field galaxies in our sample cover a similar range of [OII]λ3727 rest-frame emission line equivalent width to that observed locally, but over a much narrower luminosity range, that is, ~ 2 mag in comparison to the ~ 7 mag covered by the NFGS galaxies. Strikingly, intermediate redshift cluster galaxies seem to be mostly located in similar regions of the diagnostic diagrams as local luminous galaxies, while [OII]λ3727 equivalent widths for galaxies in the field extend to values observed locally only at much lower luminosities. As mentioned earlier, an exception to this trend is provided by two cluster galaxies with [OII]λ3727 equivalent widths higher than nearly all of our distant field galaxies.

The right panel of Fig. 3 shows the variation of [OII]λ3727 emission line rest-frame equivalent width as a function of the ionization-sensitive diagnostic ratio $O_{32} = $[OIII]$\lambda$4959, λ5007/[OII]λ3727. Intermediate redshift cluster and field galaxies are shown as in the left panel of the figure. To illustrate the effect of galaxy luminosity on O_{32}, we split the local sample of star-forming galaxies into faint ($M_B > -19.5$) and bright ($M_B \leqslant -19.5$), samples. As discussed in Mouhcine et al. (2006), the bright, star-forming field galaxies at intermediate redshifts tend to be located in the same region as *faint* local star-forming galaxies in the plot of [OII]λ3727 equivalent width versus O_{32}, and show higher ionization-sensitive diagnostic ratios (O_{32}) than are seen locally in galaxies with comparable luminosities. However, our distant, star-forming cluster galaxies preferentially inhabit the same region in the [OII]λ3727 equivalent width versus O_{32} diagram as local field galaxies with similar, bright, luminosities. Exceptions to this are the same two high [OII]λ3727 equivalent width galaxies discussed previously, and the population of high-O_{32} cluster galaxies. While the O_{32} distributions of our distant field and cluster galaxies are similar (see Fig. 2), the [OII]λ3727 equivalent widths display a strong difference. The galaxies most responsible for this difference appear to be those with $O_{32} \gtrsim 0.4$. This combination of high O_{32} and low [OII]λ3727 equivalent widths is rather more unusual in both our distant and local field samples.

The broad similarity between the observed rest-frame emission line equivalent widths and diagnostic ratios for bright, star-forming galaxies in the local field and those in intermediate-redshift clusters, suggests that the two samples span the same range of HII region physical parameters, in terms of ionizing flux, ionization parameter, and metallicity. This also indicates that the R_{23} vs. $12 + \log(O/H)$ local calibration should be valid for converting line ratios measured for distant cluster galaxies in our sample into oxygen abundances, without introducing any systematic biases.

Fig. 5 shows the relationship between galaxy luminosity and oxygen abundance for our sample of distant star-forming

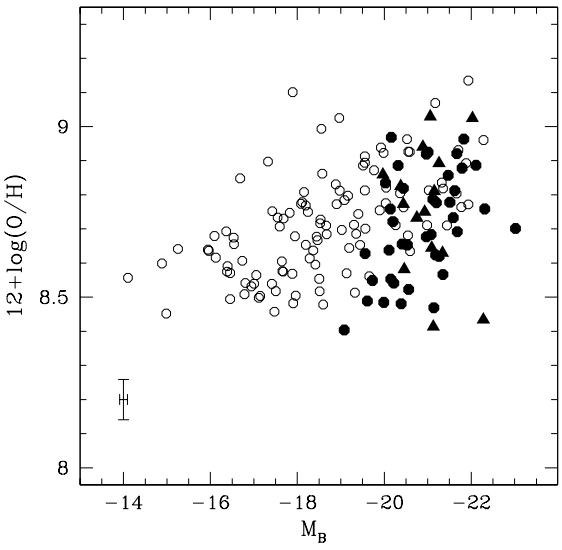

Figure 5. Luminosity–metallicity relation for our sample of intermediate redshift star-forming cluster galaxies (filled triangles), compared with a sample of intermediate redshift star-forming field galaxies (filled circles), and local star-forming galaxies from the NFGS sample (open circles).

cluster galaxies compared with the distant field and local galaxy samples. The local sample shows the well-established luminosity–metallicity relation (e.g., Skillman et al. 1989; Zaritsky et al. 1995; Richer & McCall 1995; Melbourne & Salzer 2002; Lamareille et al. 2004; Tremonti et al. 2004). As expected from Fig. 2, our distant cluster and field galaxies are distributed similarly.

The panels of Fig. 6 show the relationship of gas phase oxygen abundance versus the rest-frame equivalent width of the [OII]λ3727 emission line (left) and extinction-corrected star formation rate (right). Symbols are the same as in Fig. 5. The star formation rates of distant cluster and field galaxies are derived using Hβ luminosities, estimated using Hβ equivalent widths and B-band absolute luminosities following equation 6 of Kobulnicky & Kewley (2004). The star formation rates are then calculated following the calibration of Kennicutt (1998). The star formation rate of galaxies in the local sample is estimated using the extinction-corrected Hα luminosity following the calibration of Kennicutt (1998).

Both distant cluster and field galaxies follow similar relations between oxygen abundance and [OII]λ3727 equivalent width (an indication of star formation rate per unit luminosity) as the local sample. However, as seen above, the intermediate redshift cluster galaxies tend to have lower [OII]λ3727 equivalent widths at a given oxgen abundance than the distant field galaxies. This is most noticeable at low oxygen abundances, but does not necessarily imply a difference in slope, as we may be missing high oxygen abundance cluster galaxies with very low [OII]λ3727 equivalent widths. As anticipated from Fig. 2, there is no evidence for a difference in the distributions of our intermediate redshift cluster and field galaxies in the oxygen abundance versus star formation rate diagram.

4 DISCUSSION AND CONCLUSIONS

We have examined the [OII]λ3727, [OIII]λ4959, λ5007 and Hβ emission line equivalent widths, and resultant diagnostic diagrams, oxygen abundances and extinction-corrected star formation rates, for a sample of 17 bright ($M_B \lesssim -20$), star-forming, mostly disc, cluster galaxies at intermediate redshifts, $0.3 \lesssim z \lesssim 0.6$.

The comparison between these distant cluster galaxies and their counterparts in the coeval field, from Mouhcine et al.(2006), reveals that the properties of the interstellar gas are broadly similar for both samples. The primary difference is that the emission line equivalent widths of the cluster galaxies are, on average, significantly lower than for the field galaxies. However, a fraction of the distant cluster galaxies appear to have much higher emission line equivalent widths, comparable to the highest seen in the field. This tentatively implies a bimodality in the star formation rates per unit luminosity of distant cluster galaxies. Our luminous, star-forming, intermediate-redshift field galaxies, on the other hand, have broad, unimodal distributions, which extend smoothly to ranges observed locally only for much fainter galaxies (Mouhcine et al. 2006).

The hint of a bimodality in the star formation rates per unit luminosity of distant cluster galaxies, with the majority being suppressed, but some apparently enhanced, lends support to a mechanism for galaxy evolution in clusters which causes a temporary increase in the star formation rate of galaxies prior to a decline in their star formation. Indications of this have also been found by considering the Tully-Fisher relation of cluster and field samples from which the galaxies studied in this paper were drawn (Milvang-Jensen et al. 2003, Bamford et al. 2005). In these studies star-forming cluster galaxies were found to have, on average, brighter B-band luminosities than those in the field, at a given rotation velocity. This is suggestive of a recent enhancement of star formation for the cluster galaxies.

We have examined the oxygen abundances for our galaxies, but are unable to discriminate between our cluster and field samples in terms of their chemical and ionisation properties. This may be due to a true lack of a difference between the two samples, perhaps because the star-forming galaxies in distant clusters have recently entered the cluster environment from the field. Two galaxies in our cluster sample show oxygen abundances significantly lower, but with similar emission line equivalent widths, than what is seen locally for similar luminosities. One of these two objects has measured rotation velocity and emission scale length, i.e., $V_{\rm rot} \approx 248\,{\rm km\,s^{-1}}$ and $r_{\rm d,spec} = 7.7\,{\rm kpc}$. This object is similar to the sub-population of massive and large galaxies in the intermediate redshift field that are offset with respect to the local luminosity–metallicity relation. Given its rotation velocity and physical size, this object is likely to evolve into a massive, metal-rich galaxy in the local universe, rather than fading into a dwarf galaxy. While this galaxy is only 1σ away from the cluster redshift, it does lie at a projected distance from the cluster centre of 0.8 times the cluster virial radius, and is therefore potentially a recent arrival from the field. The other object with low oxygen abundance is at the cluster redshift and lies at a projected distance from the cluster centre of 0.3 times the cluster virial radius. It may be a recent addition to the cluster, but there is no evidence

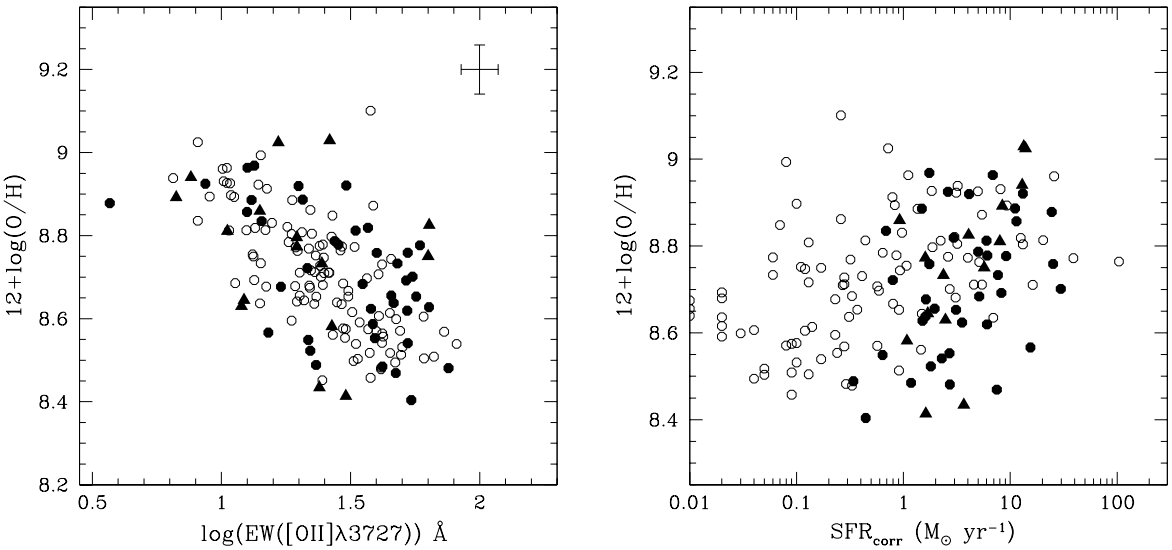

Figure 6. Plots showing the relationships between oxygen abundance and rest-frame [OII]λ3727 equivalent width *(left)*, and extinction-corrected star formation rate *(right)*. Intermediate redshift star-forming cluster/field galaxies are shown as filled triangles/circles, and the NFGS sample of local star-forming galaxies is marked by open circles.

for or against this. Alternatively, the similarities between intermediate redshift field and cluster galaxies we have found could be due to the lack of the required statistical power to measure the differences, due to our small sample size. However, we have established some upper limits on the possible differences between the samples.

The sample considered in this paper is not large or diverse enough to address the issue of differential evolution of cluster and field galaxies quantitatively. We have been forced to combine galaxies from a number of clusters with a range of redshifts and velocity dispersions, in order to produce a usefully sized sample. In doing so we have necessarily 'blurred out' any variations which may exist with respect to cluster mass and redshift. The galaxy clusters studied here are among the most massive candidates at intermediate redshifts ($\sigma_{cl} \approx 750$–1350). They are also located over a fairly narrow redshift range ($z = 0.31$–0.56). Our results and conclusions are thus restricted to massive clusters at $z \sim 0.4$.

There is as yet little constraints on the form that the variation of galaxy chemical evolutionary status takes with environment; is it a smooth transition with cluster mass, or are all galaxies in environments above a particular threshold density equally affected? An expectation for the relationship between environment and the chemical evolutionary status of its constituent galaxies may be inferred from the trends observed for star formation. The total star formation rate per cluster mass (Finn et al. 2005), the fraction of star-forming cluster galaxies, and the star formation rates of individual cluster galaxies (Poggianti et al. 2006) correlate strongly with cluster mass, in the sense that clusters with larger velocity dispersions tend to have systematically lower star-formation activity, and are populated by more passive galaxies (but see also Kodama et al. 2004b). An anti-correlation between the cluster X-ray luminosity and the total star formation rate per cluster mass (Homeier et al. 2005) offers support for the dependence of the normalized star formation rate on cluster mass. The correlation between star formation activity and cluster mass seems to be traced by both high and low redshift clusters (as suggested by Lewis et al. 2002, Gomez et al. 2003). However, Goto (2005) has found, using a sample of low redshift cluster galaxies as faint as $M_r = -20.38$, drawn from the Sloan Digital Sky Survey, that the fraction of late-type galaxies and the mass-normalized star formation rate do not significantly depend on cluster mass.

In order to fully quantify the effect of environment on the chemical evolution of galaxies, future studies must thus overcome the degenerate effects of cluster mass and redshift on galaxy properties. They will therefore require considerably larger samples than are considered here, spanning a range of cluster masses at a variety of redshifts.

Another missing piece of this puzzle is the behaviour of faint galaxies. In our sample we consider only the brightest galaxies, with $M_B \lesssim -20$. The effect of environment on the chemical evolution of galaxies as a function of galaxy luminosity and mass is unknown at intermediate redshifts. Investigating this topic must be postponed until intermediate redshift field and cluster galaxy samples are available with large quantities of star-forming galaxies spanning a range of galaxy luminosity.

REFERENCES

Baldwin J.A., Phillips M.M., Terlevich R., 1981, PASP, 93, 5

Balogh M. L., Schade D., Morris S. L., Yee H. K. C., Carlberg R. G., Ellingson E., 1998, ApJ, 504, L75

Balogh M. L., Baldry I. K., Nichol R., Miller C. Bower R., Glazebrook K., 2004, ApJ, 615, L101

Bamford S. P., Milvang-Jensen B., Aragón-Salamanca A., Simard L., 2005, MNRAS, 361, 109

Bamford S. P., Aragón-Salamanca A., Milvang-Jensen B., 2006, MNRAS, 366, 308
Beers T. C., Flynn K., Gebhardt K., 1990, AJ, 100, 32
Butcher H., Oemler A., 1978, ApJ, 219, 18
Butcher H., Oemler A., 1984, ApJ, 285, 426
Cardelli J.A., Clayton G.C., Mathis J.S., 1989, ApJ, 329, 33
Couch W.J., Sharples R.M., 1987, MNRAS, 229, 423
Cowie L.L., et al., 1997, ApJ, 481, L9
Davis M., et al., 2003, SPIE, 4834, 161
Dressler A., 1980, ApJ, 236, 351
Dressler A., Gunn J.E., 1992, ApJS, 78, 1
Dressler A., et al., 1997, ApJ, 490, 577
Ellison S. L., Kewley L. J., 2005, in "The Fabulous Destiny of Galaxies; Bridging the Past and Present", in press (astro-ph/0508627)
Finn R. A., et al., 2005, ApJ, 630, 206
Girardi M. & Mezzetti M., 2001, ApJ, 548, 79
Gómez P. L., et al., 2003, ApJ, 584, 210
Goto T., 2005, MNRAS, 356, L6
Hoekstra H., Franx M., Kuijken K., van Dokkum P. G., MNRAS, 333, 911
Homeier N. L., et al., 2005, ApJ, 621, 651
Huchra J.P., Davis M., Latham D., Tonry J. 1983, ApJS, 52, 89
Jansen R.A., Fabricant D., Franx M., Caldwell N., 2000, ApJS, 126, 331
Kashikawa N., et al., 2002, PASJ, 54, 819
Kennicutt R.C., Jr. 1998, ARA&A, 36, 189
Kewley L.J., Dopita M.A., 2002, ApJS, 142, 35
Kewley, L.J., Geller, M., & Jansen, R.A., 2004, AJ, 127, 2002
Kobulnicky H. A., Kennicutt Jr. R. C., Pizagno J. L., 1999, ApJ, 514, 544
Kobulnicky H. A., et al. 2003, ApJ, 599, 1006
Kobulnicky H. A., Phillips A. C., 2003, ApJ, 599, 1031
Kodama T., et al., 2004a, MNRAS, 350, 1005
Kodama T., et al., 2004b, MNRAS, 354, 1103
Kong X., Cheng F.Z., Weiss A., Charlot S., 2002, A&A, 396, 503
Lamareille F., Mouhcine M., Contini T., Lewis I.J., Maddox S.J., 2004, MNRAS, 350, 396
Lewis I.J., et al., 2002, MNRAS, 334, 673
Liang Y.C., Hammer F., Flores H., Gruel N., Assémat F., 2004, A&A, 417, 905
Maier C., Meisenheimer K., Hippelein H., 2004, A&A, 418, 475
McCall M.L., Rybski P.M., Shields G.A., 1985, ApJS, 57, 1
McGaugh S. S., 1991, ApJ, 380, 140
Melbourne J., Salzer J. J., 2002, AJ, 123, 2302
Milvang-Jensen B., Aragón-Salamanca A. Hau G. K. T., Jørgensen I. Hjorth J., 2003, 339L, 1
Morgan W.W., 1961, PNAS, 47, 905
Moss C., Whittle M., 1993, ApJ, 407L, 17
Moss C., Whittle M., 2000, MNRAS, 317, 667
Mouhcine M., Bamford S.P., Aragón-Salamanca A., Nakamura O., 2006, MNRAS submitted
Mouhcine, M., Lewis, I, Jones, B., Lamareille, F., Maddox, S.J., Contini, T., 2005, MNRAS, 362, 1143
Nakamura, O., Aragón-Salamanca, A., Milvang-Jensen, B., Arimoto, N., Ikuta, C., Bamford, S. P., 2006, MNRAS, 366, 144
Osterbrock D.E., 1989, Astrophysics of Gaseous Nebulae and Active Galactic Nuclei (Mill Valley: Unvi. Sci.)
Pagel B.E.J., Edmunds M.G., Blackwell D.E., Chum M.S., Smith G., 1979, MNRAS, 189, 95
Poggianti B. M., et al., 1999, ApJ, 518, 576
Poggianti B. M., et al., 2006, ApJ submitted
Postman M., Lubin L. M., Oke J.B., 2001, AJ, 122, 1125
Richer M.G., McCall M.L., 1995, ApJ, 445, 642
Salzer J.J., MacAlpine G.M., Boroson T.A., 1989, ApJS, 70, 479
Seifert W., et al., 2000, in Iye M., Moorwood, A. F., eds, Proc. SPIE Vol. 4008, Optical and IR Telescope Instrumentation and Detectors p. 96
Skillman E.D., Kennicutt R.C., Hodge P.W., 1989, ApJ, 347, 875
Smail I., et al., 1997, ApJS, 110, 213
Stasińska G., 1990, A&AS, 83, 501
Stocke J. T., et al., 1991, ApJS, 76, 813
Tremonti C.A., Heckman T.M., Kauffmann G., et al., 2004, ApJ, 613, 898
Tully R.B., Fisher J.R., 1977, A&A, 54, 661
Veilleux S., Osterbrock D. E., 1987, ApJS, 63, 295
Welch B.L., 1937, Biometrika, 29, 2057
White S.D.M, et al., 2005, A&A in press (astro-ph/0508351)
Zaritsky D., Kennicutt R.C., Huchra J.P, 1994, ApJ, 420, 87
Ziegler B.L., Böhm A., Jäger K., Heidt J., Möllenhoff C., 2003, ApJ, 598, 87

This paper has been typeset from a TEX/ LATEX file prepared by the author.